

A new equivalent friction element for analysis of cable supported structures

Renzhang Yan^{1,2a}, Zhihua Chen^{1,2b}, Xiaodun Wang^{*1,2},
Hongbo Liu^{1,2} and Xiao Xiao^{1,2}

¹ School of Civil Engineering, Tianjin University, Tianjin, 300072, China

² Key Laboratory of Coast Civil Structure and Safety, Ministry of Education,
Tianjin University, Tianjin, 300072, China

(Received February 26, 2014, Revised July 30, 2014, Accepted October 10, 2014)

Abstract. An equivalent friction element is proposed to simulate the friction in cable-strut joints. Equivalent stiffness matrixes and load vectors of the friction element are derived and are unified into patterns for FEM by defining a virtual node specially to store internal forces. Three approaches are described to verify the rationality of the new equivalent friction element: applying the new element in a cable-roller model, and numerical solutions match well with experimental results; applying the element in a continuous sliding cable model, and theoretical values, numerical and experimental results are compared; and the last is applying it in truss string structures, whose results indicate that there would be a great error if the cable of cable supported structures is simulated with discontinuous cable model which is usually adopted in traditional finite element analysis, and that the prestress loss resulted from the friction in cable-strut joints would have adverse effect on the mechanical performance of cable supported structures.

Keywords: equivalent friction element; equivalent stiffness; equivalent load; experiment; cable supported structure

1. Introduction

The cable supported structure is a new type of efficient structural system which takes advantage of the prestressing force in cables to achieve the optimization of internal force and displacement distribution of the structure (Chen 2013). In addition to experimental approach, finite element analysis with numerical models based on the computer simulation technology has been a widely adopted and effective alternative to conduct researches on cable supported structures. However, a key problem confronted with scholars around the world is how to find an appropriate method to establish a proximate numerical model that is closest to the real structure, ensuring that the actual working status of the structure could be simulated by the model more accurately. The cable, which is a key component of cable supported structures, is continuous in a structure to achieve

*Corresponding author, Associate Professor, E-mail: maodun2004@126.com

^a Ph.D. Student, E-mail: yrzsuper@tju.edu.cn

^b Professor, E-mail: zhchen@tju.edu.cn

continuous tensile forces in the structure. In previous finite element analysis, the cable is assumed to be discontinued due to cable-strut joints (Wang *et al.* 2007a, b, Zhu *et al.* 2013, Thai and Kim 2011, Li and Chan 2004). However, the adjacent cable segments on the two sides of a strut would actually slide through the joint, especially during the construction of stretching cables. Therefore, it would result in great error to simulate the cable by a discontinuous model.

To avoid the error resulted from the discontinuous model of cable, continuous model has been proposed by researchers around the world. Tang and Shen (1999) and Tang *et al.* (1997) proposed a five-node isoparametric element to simulate the continuous cable in cable supported structures. Based on catenary elements, different cable elements considering the sliding of cable are proposed by Zhang and Dong (2001), Wei (2004) and Nie *et al.* (2003) respectively. In addition, a frozen-heated method is adopted to apply virtual temperature load in order to achieve equivalent internal forces in adjacent cable segments, simulating the case of continuous cable (Cui *et al.* 2004). A three-node cable element with cable clamp is proposed by Aufaure (2000), and the sliding of cable is considered with additional generalized degrees of freedom. Zhou *et al.* (2004) put forward a three-node sliding cable element based on the same strain of cable segments, and the stiffness matrix of the element is also derived. Chen *et al.* (2010) proposed the analysis method of the sliding cable element put forward based on theories of Lagrange isoparametric element, Green strain and Cauchy stress. However, the friction between continuous cable and struts is not taken into account in the above researches. The influence of prestressing loss resulted from the friction in cable-strut joints on structural behavior is investigated by Wang *et al.* (2008), and the results indicate that the prestressing loss would cause a non-uniform internal force distribution and a 20% decline of global stability performance. Therefore, the friction loss in cable-strut joints should be taken into account in construction analysis of cable supported structures; otherwise, the bearing capacity of the structure would be overestimated. Liu *et al.* (2009) proposed an iterative method based on theories of pseudo temperature and generalized inverse in functional analysis to consider the friction loss. Zhang *et al.* (2008) proposed a modified original length method to consider the effect of friction loss. However, both two methods require a time-consuming iterative analysis by establishing equilibrium equations of friction and internal forces in cable. Wei (2006) proposed a three-node friction sliding element and derive the sliding stiffness at the support, which is, however, complex for engineers to require. The coupling degrees of freedom in cable-strut joints and variable-stiffness spring are used to simulate the friction loss by Wang *et al.* (2008). Nonetheless, detailed process of the method is not presented and the stiffness of spring is complex to determine accurately. A solid model of cable-strut joint in suspen-dome is established by Wang *et al.* (2007a, b), and the sliding friction is analyzed with nonlinear contact element. The main problems of this method are that the calculation is complicated and it can be applied in joint analysis only and not suitable to analyze the sliding of the whole cable.

Contact friction is highly nonlinear. In fact, there have been many numerical methods in geotechnical engineering field to solve contact friction between discontinuous surfaces existing in faults or fissures. A new contact friction element is proposed by Lei (Lei 2001, Lei *et al.* 1995) based on relevant researches (Katona 1983). In this method, the contact stress of joint is selected as an unknown variable, and the geometric shape of contact surface is simulated with six-node isoparametric elements. Geometric equations and static equations are included in the stiffness equation, and finally equivalent stiffness matrix is assembled into global stiffness matrix of the structure. Therefore, it is not necessary to obtain the stiffness coefficient of contact friction element, which is usually complex, thus reducing computational cost. Note that the method is proposed to solve the surface contact issues in rocks which differ from the point-line contact in

cable-strut joints of cable supported structures. However, it is indeed an efficient approach to solve issues about friction by selecting contact stress as an unknown variable and assembling geometric and static equations at the contact point into equivalent stiffness matrix of friction element. Based on the above method, a new equivalent friction element which can be applied in cable-strut joints in cable supported structures is put forward in this paper. Since it only requires judging the contact state of friction elements instead of conducting iterative analysis of cable force and friction, the amount of computational work would be reduced significantly when compared with the methods by Liu *et al.* (2009) and by Zhang *et al.* (2008).

2. Equivalent friction element

The equivalent friction element put forward in the paper is applied mainly in cable supported structures. Take a beam string structure, shown as Fig. 1, as an example to illustrate the application of the equivalent friction element. Detailed information about the contact in the cable-strut joint is shown in Fig. 2, where the joint 4 represents the lower strut joint and the joint 3 represents the cable joint contacting with the joint 4. It is a point-line contact issue when the continuous cable slides through the joint 4. Equivalent friction elements are established between the joint 3 and 4, and the tangential component and the normal component of force would exist in elements. A five-node equivalent friction element is shown in Fig. 3. Node 1 and 2 represent corresponding adjacent nodes in the cable joint, and node 3 represents the node at the contacting point in the continuous cable. An element coordinate system is defined by node 1, 2 and 3. Node 4 represents the corresponding lower strut joint, and node 5 is a virtual node to store information about internal forces of the equivalent friction element, which will be described in detail later in the paper. Coordinate values of node 1, 2, 3 and 4 are (x_1, y_1) , (x_2, y_2) , (x_3, y_3) and (x_4, y_4) respectively. Since the coordinate value of node 5 can be set randomly, it is set as the same value as node 4 in the paper.

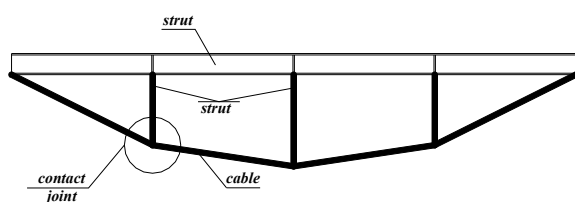


Fig. 1 Cable supported structure

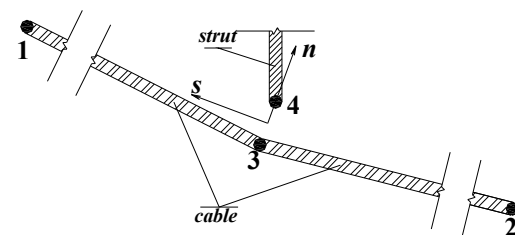


Fig. 2 Details of contact in cable-strut joint

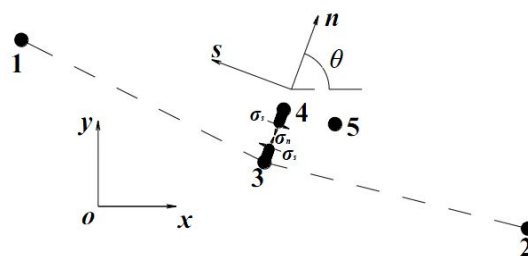


Fig. 3 Equivalent friction element

2.1 Element coordinate system

For a convenient describe of the issue, it is assumed in Fig. 3 that node 3 and node 4 are in different position, though they actually coincide with each other before the structure is subjected to external force. The n -axis is defined as the direction of normal pressure, i.e., the direction of angular bisector of adjacent cable segments. The s -axis is defined as the direction of friction, i.e., the tangential direction of the cable at node 3. An element coordinate system can be established by right-hand screw rule, and the included angle between the n -axis and the x -axis is assumed as θ , shown as in Fig. 3. In the element, the positive internal force is defined if node 3 and node 4 move apart due to the force, similar to the way that the positive force is defined in the link element. In the element coordinate system, the projections of n -axis on the x -axis and y -axis are shown as Eq. (1).

$$\begin{cases} \cos \theta = \text{norm}(\bar{e}_{31} + \bar{e}_{32}) \cdot [1 \ 0]^T \\ \sin \theta = \text{norm}(\bar{e}_{31} + \bar{e}_{32}) \cdot [0 \ 1]^T \end{cases} \quad (1)$$

Where, $\text{norm}(\dots)$ signify a unit vector standardized from the vector within parentheses; \bar{e}_{31} and \bar{e}_{32} represent the unit vector along the direction of node 3 to 1 and node 3 to 2 respectively. And \bar{e}_{31} and \bar{e}_{32} are shown as below.

$$\bar{e}_{31} = \frac{1}{\sqrt{(x_1 - x_3)^2 + (y_1 - y_3)^2}} \cdot [x_1 - x_3 \quad y_1 - y_3],$$

$$\bar{e}_{32} = \frac{1}{\sqrt{(x_2 - x_3)^2 + (y_2 - y_3)^2}} \cdot [x_2 - x_3 \quad y_2 - y_3].$$

2.2 Equilibrium equation of internal stress and nodal load

In general, the nodal displacement is selected as the unknown variable in finite element analysis, and the relation of the nodal load and nodal displacement is established in element stiffness matrix. However, the internal stress is selected as the unknown variable in equivalent friction element, and the relation of nodal load and internal stress should be established first. In an equivalent friction element, node 1 and node 2 are used to determine the position of the element, and node 5 is a virtual node, and only node 3 and node 4 have certain physical interpretations. Hence, the nodal load can be expressed as $\{F_{3x}, F_{3y}, F_{4x}, F_{4y}\}^T$ in global coordinate system. Force diagrams of node 3 and node 4 are shown in Fig. 4, where σ_n and σ_s represent internal stresses in equivalent friction element along normal and tangential directions respectively. According to equilibrium equations at node 3 and node 4, Eq. (2) and Eq. (3) are established in x -axis and y -axis respectively, and Eq. (4) is a matrix form of Eq. (2) and Eq. (3). Considering that nodes in the structure are actually not subjected to external loads, Eq. (4) is transformed into Eq. (5), thus yielding the equilibrium equation of internal stress and nodal load in an equivalent friction element.

$$\begin{cases} F_{3x} + \sigma_n \cdot \cos \theta - \sigma_s \cdot \sin \theta = 0 \\ F_{3y} + \sigma_n \cdot \sin \theta + \sigma_s \cdot \cos \theta = 0 \end{cases} \quad (2)$$

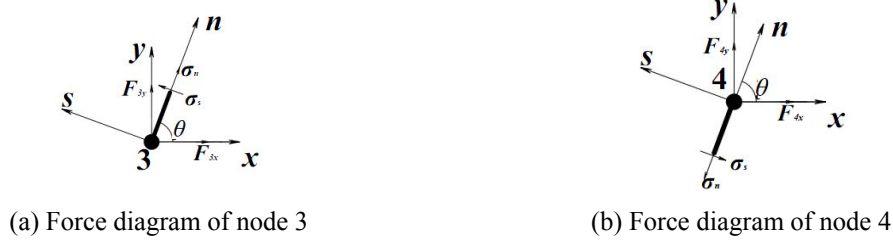


Fig. 4 Force diagrams of nodes in equivalent friction element

$$\begin{cases} F_{4x} - \sigma_n \cdot \cos \theta + \sigma_s \cdot \sin \theta = 0 \\ F_{4y} - \sigma_n \cdot \sin \theta - \sigma_s \cdot \cos \theta = 0 \end{cases} \quad (3)$$

$$\begin{bmatrix} -\cos \theta & \sin \theta \\ -\sin \theta & -\cos \theta \\ \cos \theta & -\sin \theta \\ \sin \theta & \cos \theta \end{bmatrix} \cdot \begin{Bmatrix} \sigma_n \\ \sigma_s \end{Bmatrix} = \begin{Bmatrix} F_{3x} \\ F_{3y} \\ F_{4x} \\ F_{4y} \end{Bmatrix} \quad (4)$$

$$\begin{bmatrix} -\cos \theta & \sin \theta \\ -\sin \theta & -\cos \theta \\ \cos \theta & -\sin \theta \\ \sin \theta & \cos \theta \end{bmatrix} \cdot \begin{Bmatrix} \sigma_n \\ \sigma_s \end{Bmatrix} = \begin{Bmatrix} 0 \\ 0 \\ 0 \\ 0 \end{Bmatrix} \quad (5)$$

2.3 Constraint equations

The internal force vector of the equivalent friction element at the end of any load step k can be expressed as Eq. (6), and the displacement vectors of node 3 and node 4 along coordinate axes are shown as Eq. (7), where the superscript k signifies the load step considered, and subscripts n and s signify directions along n -axis and s -axis respectively. Relative displacements of node 3 and node 4 along n -axis and s -axis can be determined by Eq. (8).

The displacement vectors of node 3 and node 4 are shown as Eq. (9). The relationship of the nodal displacement for node i ($i = 3, 4$) in element coordinate system and in global coordinate system is presented in Fig. 5. The relationship shown in Fig. 5 can be expressed as Eqs. (10) and (11). Eq. (12), describing the relationship of relative displacement of node 3 and node 4 in element coordinate system and in global coordinate system, can be derived by substituting Eqs. (10) and

(11) into Eq. (8). Substituting $L = \begin{bmatrix} -\cos \theta & -\sin \theta & \cos \theta & \sin \theta \\ \sin \theta & -\cos \theta & -\sin \theta & \cos \theta \end{bmatrix}$ and Eq. (9) into Eq. (12) yields Eq. (13).

$$\sigma^k = \begin{Bmatrix} \sigma_n^k \\ \sigma_s^k \end{Bmatrix} \quad (6)$$

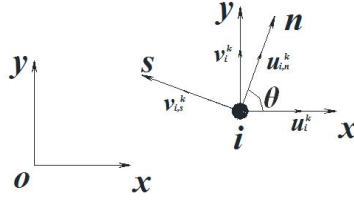


Fig. 5 Relationship of nodal displacement in element coordinate system and in global coordinate system

$$u^k = \{u_{3,n}^k \quad v_{3,s}^k \quad u_{4,n}^k \quad v_{4,s}^k\}^T \tag{7}$$

$$\Delta u^k = \begin{Bmatrix} u_n^k \\ v_s^k \end{Bmatrix} = \begin{Bmatrix} u_{4,n}^k - u_{3,n}^k \\ v_{4,s}^k - v_{3,s}^k \end{Bmatrix} \tag{8}$$

where:

- u_n^k – relative displacement of node 3 and node 4 in equivalent friction element (EFE) along n -axis at the end of load step k ;
- $u_{3(4),s}^k$ – displacement of node 3 or node 4 in EFE along s -axis at the end of load step k ;
- v_n^k – relative displacement of node 3 and node 4 in EFE along n -axis at the end of load step k ;
- $v_{3(4),s}^k$ – displacement of node 3 or node 4 in EFE along s -axis at the end of load step k .

$$U^k = \{u_3^k \quad v_3^k \quad u_4^k \quad v_4^k\}^T \tag{9}$$

$$\begin{cases} u_{3,n}^k = u_3^k \cdot \cos \theta + v_3^k \cdot \sin \theta \\ v_{3,s}^k = u_3^k \cdot (-\sin \theta) + v_3^k \cdot \cos \theta \end{cases} \tag{10}$$

$$\begin{cases} u_{4,n}^k = u_4^k \cdot \cos \theta + v_4^k \cdot \sin \theta \\ v_{4,s}^k = u_4^k \cdot (-\sin \theta) + v_4^k \cdot \cos \theta \end{cases} \tag{11}$$

$$\begin{aligned} \Delta u^k &= \begin{Bmatrix} u_3^k \cdot (-\cos \theta) + v_3^k \cdot (-\sin \theta) + u_4^k \cdot \cos \theta + v_4^k \cdot \sin \theta \\ u_3^k \cdot \sin \theta + v_3^k \cdot (-\cos \theta) + u_4^k \cdot (-\sin \theta) + v_4^k \cdot \cos \theta \end{Bmatrix} \\ &= \begin{bmatrix} -\cos \theta & -\sin \theta & \cos \theta & \sin \theta \\ \sin \theta & -\cos \theta & -\sin \theta & \cos \theta \end{bmatrix} \cdot \begin{bmatrix} u_3^k \\ v_3^k \\ u_4^k \\ v_4^k \end{bmatrix} \end{aligned} \tag{12}$$

$$\Delta u^k = L \cdot U^k \tag{13}$$

Where L is as shown in Eq. (11).

$$L = \begin{bmatrix} -\cos\theta & -\sin\theta & \cos\theta & \sin\theta \\ \sin\theta & -\cos\theta & -\sin\theta & \cos\theta \end{bmatrix} \quad (14)$$

There are only three types of contact between the continuous cable and lower strut joints: fixed, sliding and separated, corresponding to different constraint equations respectively. The fixed state means that two neighboring nodes in the equivalent friction element are static relatively to each other when the external force is less than the maximum static friction in the contact point, which is similar to the case where the two nodes are fixed together. The fixed state is used in the paper to describe this specific contact, in which no relative displacement exists between the two neighboring nodes, i.e., relative displacements of node 3 and node 4 in the direction of n -axis and s -axis are both 0; in the case of sliding contact, relative displacement of node 3 and node 4 along n -axis is 0, and the tangential stress $\sigma_s = T$; in the case of separation, the normal stress and the tangential stress are N and T respectively, i.e., $\sigma_n = N$ and $\sigma_s = T$. Hence, the contact state of the element can be obtained by relative displacements of node 3 and node 4 along the element coordinate axes and (or) stresses of the element, and each contact state can be determined by two constraint conditions. Different constraint equations in different contact state of the equivalent friction element can be written as a unified expression as Eq. (15), where L' is the relative displacement constraint matrix; R' is the stress constraint matrix; a^* , b^* are corresponding values of displacements and (or) stress, related to the contact condition in the load step $(k-1)$, and specific values are shown in Table 1.

$$[L' \quad R'] \cdot \begin{bmatrix} U^k \\ \sigma^k \end{bmatrix} = \begin{Bmatrix} a^* \\ b^* \end{Bmatrix} \quad (15)$$

(1) Fixed state

In the fixed state, the relative normal displacement u_n^k and tangential displacement v_s^k are all zero. The contact state would not be affected by the change of element stress. Particularly, if the joint is in separated state in the load step $k-1$, $u_n^k = -u_n^{k-1}$, $v_s^k = -v_s^{k-1}$.

$$L' = L = \begin{bmatrix} -\cos\theta & -\sin\theta & \cos\theta & \sin\theta \\ \sin\theta & -\cos\theta & -\sin\theta & \cos\theta \end{bmatrix} \quad (16)$$

Table 1 Constraint values in different contact conditions

Load step	k	Fixed	Sliding	Separated
	$k-1$			
Fixed		$a^* = u_n^{k*} = 0$ $b^* = v_s^{k*} = 0$	$a^* = u_n^k = 0$ $b^* = T = f^k - \sigma_s^{k-1}$	$a^* = N = -\sigma_n^{k-1}$ $b^* = T = -\sigma_s^{k-1}$
Sliding		$a^* = u_n^{k*} = 0$ $b^* = v_s^{k*} = 0$	$a^* = u_n^k = 0$ $b^* = T = f^k - \sigma_s^{k-1}$	$a^* = N = -\sigma_n^{k-1}$ $b^* = T = -\sigma_s^{k-1}$
Separated		$a^* = u_n^{k*} = -u_n^{k-1}$ $b^* = v_s^{k*} = v_s^k \left \frac{u_n^{k-1}}{u_n^k} \right $	$a^* = u_n^{k*} = -u_n^{k-1}$ $b^* = T = f^k$	$a^* = N = 0$ $b^* = T = 0$

$$R' = \begin{bmatrix} 0 & 0 \\ 0 & 0 \end{bmatrix} \tag{17}$$

$$\begin{Bmatrix} a^* \\ b^* \end{Bmatrix} = \begin{Bmatrix} u_n^{k*} \\ v_n^{k*} \end{Bmatrix} \tag{18}$$

Substituting Eq.s (9), (16)~(18) into Eq. (15) yields the constraint equation in the fixed state as Eq. (19).

$$\begin{bmatrix} -\cos\theta & -\sin\theta & \cos\theta & \sin\theta & 0 & 0 \\ \sin\theta & -\cos\theta & -\sin\theta & \cos\theta & 0 & 0 \end{bmatrix} \begin{bmatrix} u_3^k \\ v_3^k \\ u_4^k \\ v_4^k \\ \sigma_n^k \\ \sigma_s^k \end{bmatrix} = \begin{Bmatrix} u_n^{k*} \\ v_n^{k*} \end{Bmatrix} \tag{19}$$

(2) Sliding state

In the case of sliding state, the relative normal displacement between node 3 and node 4 $u_n^k = 0$; the relative tangential displacement can be any value due to the sliding in tangential direction. The tangential stress σ_s^k is a constant value T , which is determined by the maximum friction f^k and the tangential stress σ_s^{k-1} in the last load step $k-1$. Specific values of T are shown in Table 1, and the calculation of f^k is shown as Eq. (24). Substituting Eqs. (9), (20)~(22) into Eq. (15) yields the constraint equation in the sliding state as Eq. (23).

$$L' = \begin{bmatrix} l_n \\ 0 \end{bmatrix} = \begin{bmatrix} -\cos\theta & -\sin\theta & \cos\theta & \sin\theta \\ 0 & 0 & 0 & 0 \end{bmatrix} \tag{20}$$

$$R' = \begin{bmatrix} 0 & 0 \\ 0 & 1 \end{bmatrix} \tag{21}$$

$$\begin{Bmatrix} a^* \\ b^* \end{Bmatrix} = \begin{Bmatrix} u_n^k \\ \sigma_s^k \end{Bmatrix} = \begin{Bmatrix} 0 \\ T \end{Bmatrix} \tag{22}$$

$$\begin{bmatrix} -\cos\theta & -\sin\theta & \cos\theta & \sin\theta & 0 & 0 \\ 0 & 0 & 0 & 0 & 0 & 1 \end{bmatrix} \begin{bmatrix} u_3^k \\ v_3^k \\ u_4^k \\ v_4^k \\ \sigma_n^k \\ \sigma_s^k \end{bmatrix} = \begin{Bmatrix} 0 \\ T \end{Bmatrix} \tag{23}$$

$$f^k = \begin{cases} \mu |\sigma_n^k| & \sigma_s^k \geq 0 \\ -\mu |\sigma_n^k| & \sigma_s^k < 0 \end{cases} \quad (24)$$

(3) Separated state

In the case of separated state, free relative displacements in both normal and tangential directions are generated in node 3 and node 4, and stresses in normal and tangential directions are constant value. Substituting Eq. (9), Eqs. (25)~(27) into Eq. (15) yields the constraint equation in the separated state as Eq. (28). Specific values of N is shown in Table 1.

$$L' = \begin{bmatrix} 0 & 0 & 0 & 0 \\ 0 & 0 & 0 & 0 \end{bmatrix} \quad (25)$$

$$R' = \begin{bmatrix} 1 & 0 \\ 0 & 1 \end{bmatrix} \quad (26)$$

$$\begin{Bmatrix} a^* \\ b^* \end{Bmatrix} = \begin{Bmatrix} \sigma_n^k \\ \sigma_s^k \end{Bmatrix} = \begin{Bmatrix} N \\ T \end{Bmatrix} \quad (27)$$

$$\begin{bmatrix} 0 & 0 & 0 & 0 & 1 & 0 \\ 0 & 0 & 0 & 0 & 0 & 1 \end{bmatrix} \begin{bmatrix} u_3^k \\ v_3^k \\ u_4^k \\ v_4^k \\ \sigma_n^k \\ \sigma_s^k \end{bmatrix} = \begin{Bmatrix} N \\ T \end{Bmatrix} \quad (28)$$

2.4 Equivalent stress-load equation

As mentioned above, the element stress is selected as the unknown variable in the equivalent friction element, and the equilibrium equation of element stress and nodal load is discussed in Section 2.2. Note that the stress in tangential or normal direction is constant in the sliding or separated state, hence necessary adjustments of Eq. (5) should be considered in the three constraint conditions in order to introduce stress constraint values into Eq. (5) and at the same time maintain

the form of unknown variables in Eq. (5) as $\begin{Bmatrix} \sigma_n^k \\ \sigma_s^k \end{Bmatrix}$.

(1) Fixed state

In the fixed state, Eq. (5) maintains the same since there is no stress constraint. Nonetheless, for

the convenience of establishment of equivalent stiffness matrix of the element, Eq. (29) is yielded by adjusting the form of unknown variable vector in Eq. (5) to that as in Eq. (15), where

$$\begin{bmatrix} 0 & 0 & 0 & 0 & -\cos\theta & \sin\theta \\ 0 & 0 & 0 & 0 & -\sin\theta & -\cos\theta \\ 0 & 0 & 0 & 0 & \cos\theta & -\sin\theta \\ 0 & 0 & 0 & 0 & \sin\theta & \sin\theta \end{bmatrix}$$

is the equivalent stress-load matrix of the equivalent friction

element, and $\begin{Bmatrix} 0 \\ 0 \\ 0 \\ 0 \end{Bmatrix}$ is the equivalent load vector in the fixed state.

$$\begin{bmatrix} 0 & 0 & 0 & 0 & -\cos\theta & \sin\theta \\ 0 & 0 & 0 & 0 & -\sin\theta & -\cos\theta \\ 0 & 0 & 0 & 0 & \cos\theta & -\sin\theta \\ 0 & 0 & 0 & 0 & \sin\theta & \sin\theta \end{bmatrix} \cdot \begin{Bmatrix} u_3^k \\ v_3^k \\ u_4^k \\ v_4^k \\ \sigma_n^k \\ \sigma_s^k \end{Bmatrix} = \begin{Bmatrix} 0 \\ 0 \\ 0 \\ 0 \end{Bmatrix} \tag{29}$$

(2) Sliding state

In the sliding state, substituting $\sigma_s^k = T$ into Eq. (5) yields Eq. (30), then moving T to the right of equation yields Eq. (31). Eq. (32) can be obtained by the same way as Eq. (29), where

$$\begin{bmatrix} 0 & 0 & 0 & 0 & -\cos\theta & 0 \\ 0 & 0 & 0 & 0 & -\sin\theta & 0 \\ 0 & 0 & 0 & 0 & \cos\theta & 0 \\ 0 & 0 & 0 & 0 & \sin\theta & 0 \end{bmatrix}$$

is the equivalent stress-load matrix, and $\begin{Bmatrix} -T \cdot \sin\theta \\ T \cdot \cos\theta \\ T \cdot \sin\theta \\ -T \cdot \cos\theta \end{Bmatrix}$ is the equivalent

load vector in the sliding state.

$$\begin{bmatrix} -\cos\theta & \sin\theta \\ -\sin\theta & -\cos\theta \\ \cos\theta & -\sin\theta \\ \sin\theta & \cos\theta \end{bmatrix} \cdot \begin{Bmatrix} \sigma_n^k \\ T \end{Bmatrix} = \begin{Bmatrix} 0 \\ 0 \\ 0 \\ 0 \end{Bmatrix} \tag{30}$$

$$\begin{bmatrix} -\cos\theta & 0 \\ -\sin\theta & 0 \\ \cos\theta & 0 \\ \sin\theta & 0 \end{bmatrix} \cdot \begin{Bmatrix} \sigma_n^k \\ \sigma_s^k \end{Bmatrix} = \begin{Bmatrix} -T \cdot \sin\theta \\ T \cdot \cos\theta \\ T \cdot \sin\theta \\ -T \cdot \cos\theta \end{Bmatrix} \tag{31}$$

$$\begin{bmatrix} 0 & 0 & 0 & 0 & -\cos\theta & 0 \\ 0 & 0 & 0 & 0 & -\sin\theta & 0 \\ 0 & 0 & 0 & 0 & \cos\theta & 0 \\ 0 & 0 & 0 & 0 & \sin\theta & 0 \end{bmatrix} \begin{Bmatrix} u_3^k \\ v_3^k \\ u_4^k \\ v_4^k \\ \sigma_n^k \\ \sigma_s^k \end{Bmatrix} = \begin{Bmatrix} -T \cdot \sin\theta \\ T \cdot \cos\theta \\ T \cdot \sin\theta \\ -T \cdot \cos\theta \end{Bmatrix} \quad (32)$$

(3) Separated state

Similarly, Eq. (33) can be yielded by substituting $\sigma_n^k = N$, $\sigma_s^k = T$ into Eq. (5), and moving N and T to the right of the equation. Then we can get the the equivalent stress-load matrix and the equivalent load vector in the separated state.

$$\begin{bmatrix} 0 & 0 & 0 & 0 & 0 & 0 \\ 0 & 0 & 0 & 0 & 0 & 0 \\ 0 & 0 & 0 & 0 & 0 & 0 \\ 0 & 0 & 0 & 0 & 0 & 0 \end{bmatrix} \begin{Bmatrix} u_3^k \\ v_3^k \\ u_4^k \\ v_4^k \\ \sigma_n^k \\ \sigma_s^k \end{Bmatrix} = \begin{Bmatrix} N \cdot \cos\theta - T \cdot \sin\theta \\ N \cdot \sin\theta + T \cdot \cos\theta \\ -N \cdot \cos\theta + T \cdot \sin\theta \\ -N \cdot \sin\theta - T \cdot \cos\theta \end{Bmatrix} \quad (33)$$

2.5 Element equivalent stiffness matrix and equivalent total load vector

Constraint equations and equivalent stress – load equations in different contact conditions are derived in Section 2.3 and 2.4 respectively. These equations can be unified into one expression, yielding the equivalent equilibrium equation of the equivalent friction element.

(1) Fixed state

Eq. (34) is yielded by unifying Eq. (29) and Eq. (19). Equivalent stiffness matrix and equivalent total load vector in the fixed state are shown as Eq. (35) and Eq. (36) respectively.

$$\begin{bmatrix} 0 & 0 & 0 & 0 & -\cos\theta & \sin\theta \\ 0 & 0 & 0 & 0 & -\sin\theta & -\cos\theta \\ 0 & 0 & 0 & 0 & \cos\theta & -\sin\theta \\ 0 & 0 & 0 & 0 & \sin\theta & \sin\theta \\ -\cos\theta & -\sin\theta & \cos\theta & \sin\theta & 0 & 0 \\ \sin\theta & -\cos\theta & -\sin\theta & \cos\theta & 0 & 0 \end{bmatrix} \begin{Bmatrix} u_3^k \\ v_3^k \\ u_4^k \\ v_4^k \\ \sigma_n^k \\ \sigma_s^k \end{Bmatrix} = \begin{Bmatrix} 0 \\ 0 \\ 0 \\ 0 \\ 0 \\ 0 \end{Bmatrix} \quad (34)$$

$$K_1 = \begin{bmatrix} 0 & 0 & 0 & 0 & -\cos\theta & \sin\theta \\ 0 & 0 & 0 & 0 & -\sin\theta & -\cos\theta \\ 0 & 0 & 0 & 0 & \cos\theta & -\sin\theta \\ 0 & 0 & 0 & 0 & \sin\theta & \sin\theta \\ -\cos\theta & -\sin\theta & \cos\theta & \sin\theta & 0 & 0 \\ \sin\theta & -\cos\theta & -\sin\theta & \cos\theta & 0 & 0 \end{bmatrix} \quad (35)$$

$$f_1 = \begin{Bmatrix} 0 \\ 0 \\ 0 \\ 0 \\ 0 \\ 0 \end{Bmatrix} \quad (36)$$

(2) Sliding state

Similarly, unifying Eqs. (32) and (23) yields Equivalent stiffness matrix in the sliding state as Eq. (37). Equivalent total load vector is shown as Eq. (38).

$$K_2 = \begin{bmatrix} 0 & 0 & 0 & 0 & -\cos\theta & 0 \\ 0 & 0 & 0 & 0 & -\sin\theta & 0 \\ 0 & 0 & 0 & 0 & \cos\theta & 0 \\ 0 & 0 & 0 & 0 & \sin\theta & 0 \\ -\cos\theta & -\sin\theta & \cos\theta & \sin\theta & 0 & 0 \\ 0 & 0 & 0 & 0 & 0 & 1 \end{bmatrix} \quad (37)$$

$$f_2 = \begin{Bmatrix} -T \cdot \sin\theta \\ T \cdot \cos\theta \\ T \cdot \sin\theta \\ -T \cdot \cos\theta \\ 0 \\ T \end{Bmatrix} \quad (38)$$

(3) Separated state

Unifying Eqs. (33) and (28) yields Equivalent stiffness matrix in the sliding state as Eq. (39). Equivalent total load vector is shown as Eq. (40).

$$K_3 = \begin{bmatrix} 0 & 0 & 0 & 0 & 0 & 0 \\ 0 & 0 & 0 & 0 & 0 & 0 \\ 0 & 0 & 0 & 0 & 0 & 0 \\ 0 & 0 & 0 & 0 & 0 & 0 \\ 0 & 0 & 0 & 0 & 1 & 0 \\ 0 & 0 & 0 & 0 & 0 & 1 \end{bmatrix} \quad (39)$$

$$f_3 = \begin{Bmatrix} N \cdot \cos \theta - T \cdot \sin \theta \\ N \cdot \sin \theta + T \cdot \cos \theta \\ -N \cdot \cos \theta + T \cdot \sin \theta \\ -N \cdot \sin \theta - T \cdot \cos \theta \\ N \\ T \end{Bmatrix} \quad (40)$$

Equivalent stiffness matrix and equivalent total load vector of the equivalent friction element in three contact conditions are obtained as above. The unknown variables in equivalent equilibrium equations of equivalent friction element are displacements of node 3 and node 4 along *x*-axis and *y*-axis and element stress. The displacement in *x*- or *y*-axis is identical to that of general finite element. Virtual node 5 is defined to storage internal force (stress) of equivalent friction element. The stiffness matrix of equivalent friction element has six degrees of freedom of nodes, including degrees of freedom of node 3 in *x*-axis and *y*-axis, degrees of freedom of node 4 in *x*-axis and *y*-axis, internal force of equivalent friction element in *n*-axis (replaced by degree of freedom of node 5 in *x*-axis) and internal force of equivalent friction element in *s*-axis (replaced by degree of freedom of node 5 in *y*-axis). The stiffness matrix of equivalent friction element can be assembled with other elements into total stiffness matrix.

3. Calculation procedure using equivalent friction element

When equivalent friction element is adopted to simulate the friction in cable-strut joints, the correct solution can be obtained by several iterations. The calculation in each load step is based on the contact condition obtained in the last load step. In other words, $\{\Delta u^{k-1}\}$ and $\{\sigma^{k-1}\}$ at the end of load step (*k* - 1) has been determined prior to the load step *k*. Particularly, in the load step 1, since the whole structure is not subjected to external force, it is assumed that all the equivalent friction elements are in fixed state at the end of the load step “0” and that the values of internal forces are 0 and node 3 and node 4 are in the same position, i.e., $\{\Delta u^0\} = \{0, 0\}^T$, $\{\sigma^0\} = \{0, 0\}^T$. In detailed calculation, the equivalent friction element is assumed to be in a certain contact state. The corresponding equivalent stiffness matrix and equivalent total load vector of the element can be obtained according to Eqs. (34)~(40) and Table 1. A trial solution can be obtained with the global stiffness matrix and the total load vector. The contact state in the trial solution is checked with Table 2: if the check result is consistent with the assumption, continue the calculation to the next load step; otherwise, take the check result as the new assumption of contact state and repeat

the calculation in the current step until the check result is consistent with the assumption. The detailed calculation process is shown in Fig. 6.

Table 2 Check list of trial solution during iteration within load step

Iterations	i	Fixed	Sliding	Separated
	$i - 1$			
Fixed		$\sigma_n^k < 0, \sigma_s^k < f^k$	$\sigma_n^k < 0, \sigma_s^k < f^k$	$\sigma_n^k > 0$
Sliding		$\sigma_n^k < 0,$ $(v_s^k - v_s^{k-1}) \cdot f^k < 0$	$\sigma_n^k < 0,$ $(v_s^k - v_s^{k-1}) \cdot f^k > 0$	$\sigma_n^k > 0$
Separated		$u_n^k < 0$		$u_n^k > 0$

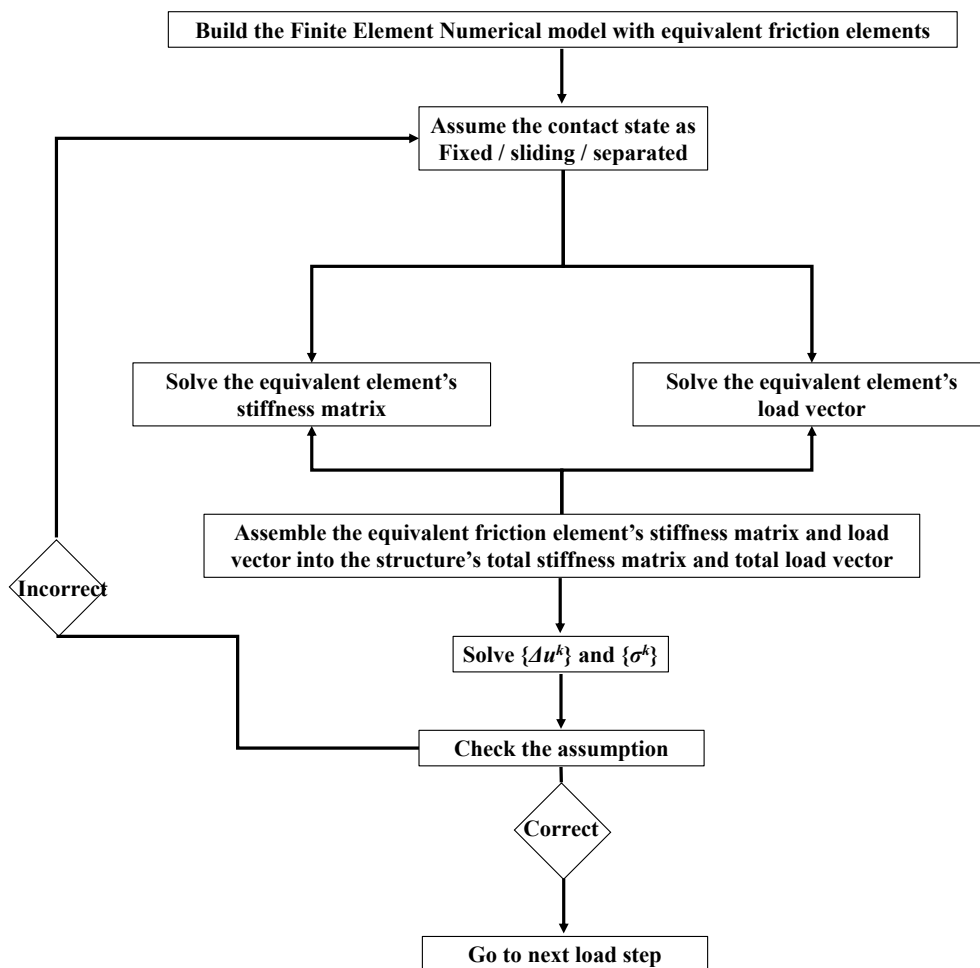


Fig. 6 Calculation process diagram

4. Application of equivalent friction element

4.1 Cable-roller model

4.1.1 Numerical model

Internal forces of the adjacent cable segments on the two sides of a joint are related to the coefficient of friction of the cable and the roller. As is shown in Fig. 7, the cable on one side of the roller is hinged, and the other side is hinged with the strut. The equivalent friction element is established in the contact point of the cable and roller. In addition, an external force $F_y = 1$ kN is applied in order to ensure the tension in cable and restrain the nodal displacement in x -axis. A finite element numerical model of equivalent friction element is established with Matlab, with $E = 2 \times 10^5$ N/mm², $A = 100$ mm² for the cable and strut. Cable forces are calculated with different coefficient of friction between cable and roller respectively: $\mu = 0$ (i.e., no friction), $\mu = 0.1$, $\mu = 0.5$ and $\mu = 2.42$. The coefficient of friction $\mu = 2.42$ is derived from the internal friction angle of the cable and roller which is 67.5° , therefore $\mu = \tan 67.5^\circ$. The calculation results are shown in Table 3.

It is indicated in Table 3 that cable forces of adjacent cable segments on the two sides of the roller are the same in the case of $\mu = 0$ (no friction exists between the cable and roller); in the case of $\mu = 2.42$ when it is just impossible for the cable to slide, the cable force could not transfer to the other side of the roller, which satisfies well with the actual case; in the case of $0 < \mu < 2.42$, there would be loss in cable force due to the friction, and a larger coefficient of friction would result in greater frictional loss.

4.1.2 Experiment of rolling cable-strut joint

Frictional loss in the process of stretching circumferential cables would be reduced significantly when rolling cable-strut joints are adopted in suspen-dome structures (Wu 2010). Relevant experimental researches have conducted in our previous work to investigate the loss of cable force on the two sides of the joint. A rolling cable-strut joint is shown in Fig. 8. The roller of

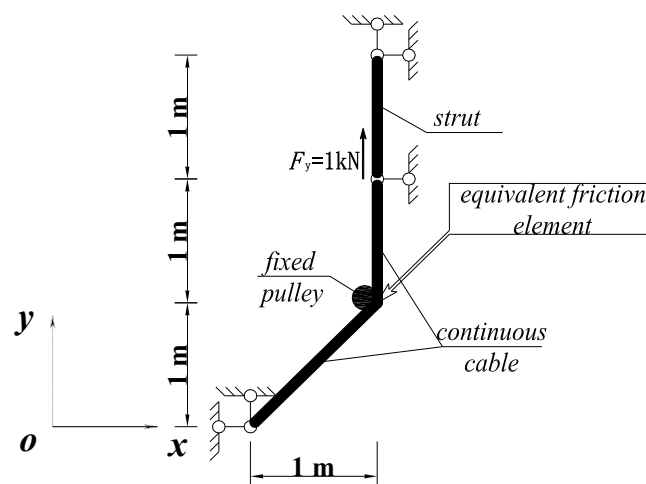


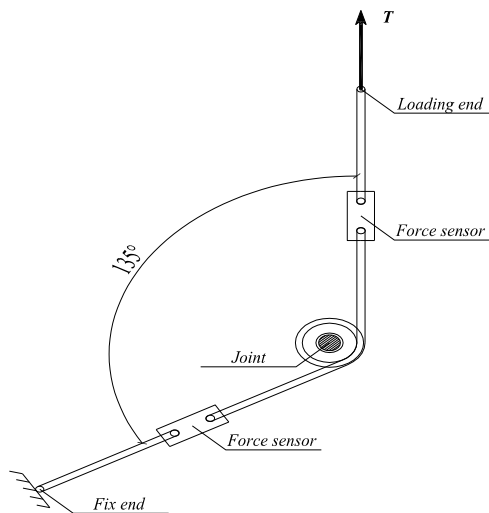
Fig. 7 Cable-roller model

Table 3 Calculation results

Friction coefficient μ	0	0.1	0.5	2.42
Internal force / N				
Frictional force f / N	0	22.3	108.7	461.9
Normal pressure N / N	-224.2	-222.6	-216.4	-191.3



Fig. 8 Rolling cable-strut joint



(a) Test model



(b) Test scene

Fig. 9 Test of stretching cable

Table 4 Results

Case	Cable force in loading end T_1 (kN)	Cable force in fixed end T_2 (kN)	Friction coefficient μ	Numerical values T_2 (kN)
Original state	40.00	33.35	0.1675	33.4
Teflon layer assembled	40.00	35.66	0.1060	35.7
Roller and pivot welded	40.00	31.34	0.2243	31.3

Note:
$$\mu = \frac{(T_1 - T_2) \cdot \sin 67.5^\circ}{(T_1 + T_2) \cdot \cos 67.5^\circ}$$

the joint is designed to reduce the friction as the roller would rotate with the sliding of the cable. Fig. 9 shows the test we have done before, with one end of the cable connected with the loading device and the other end fixed in the frame.

Internal forces of the two cable segments are determined by the rolling state of roller. Cable forces of the two cable segments are obtained in the test, considering three different conditions: free sliding of the roller and the pivot (also called the original state in the paper), a Teflon layer between the roller and the pivot, and the roller and the pivot welded together. Cable forces at two ends of the cable when the cable is stretched with the maximum designed load are listed in Table 4.

It is shown in Table 4 that test results of cable force at the fixed end coincide with results obtained with the numerical model. It should be noted that the conclusion is based on the fact that the coefficient of friction is obtained in experiment. Therefore, the effect of friction on cable force and the structure could be evaluated by numerical simulation with equivalent friction elements if the coefficient of friction of the joint could be obtained accurately in practical engineering.

4.2 Continuous sliding cable

The application of the equivalent friction element in the cable-roller model is proved feasible in Section 4.1. A continuous sliding cable model, which is composed of several cable-roller models, is designed to investigate the feasibility of the equivalent friction element further. Segment numbers and included angles of adjacent cable segments are shown in Fig. 10.

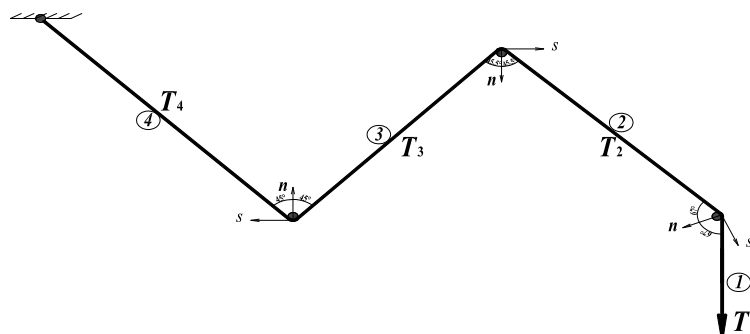


Fig. 10 A sketch of continuous sliding cable

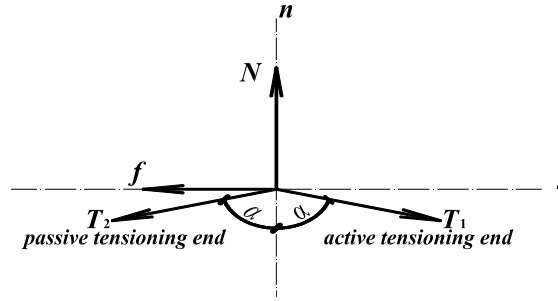


Fig. 11 Calculation diagram

4.2.1 Theoretical solution

The calculation diagram of a continuous sliding cable at a turning point is shown in Fig. 11. Equilibrium equations of forces in n -axis and s -axis are shown in Eq. (41). Eq. (43) can be derived from Eqs. (41) and (42) which indicates the relation of sliding friction and pressure. As is shown in Fig. 14, theoretical values T_2 , T_3 and T_4 can be obtained by substituting $\mu = 0.26$ (experimental result) into Eq. (43).

$$\begin{cases} f + T_2 \cdot \sin \alpha = T_1 \cdot \sin \alpha \\ N = T_1 \cdot \cos \alpha + T_2 \cdot \cos \alpha \end{cases} \quad (41)$$

$$f = \mu \cdot N \quad (42)$$

$$T_2 = T_1 \cdot \frac{\tan \alpha - \mu}{\tan \alpha + \mu} \quad (43)$$

4.2.2 Results obtained with equivalent friction element

The numerical model of a continuous sliding cable is established with Matlab software. Equivalent friction elements are established in each turning point of the cable. The coefficient of friction is $\mu = 0.26$ (experimental result), and the sectional area and modulus of elasticity of the cable are $A = 19.6 \text{ mm}^2$ and $E = 2.0 \times 10^5 \text{ N/mm}^2$. Cable forces of cable segments are shown in Fig. 14, which is called numerical solutions in the paper.

4.2.3 Experiment of continuous sliding cable

A continuous sliding cable model is made as shown in Fig. 12. $\Phi 5$ wire rope is adopted in the



Fig. 12 Continuous sliding cable in the test



Fig. 13 Connection of the cable and a dynamometer

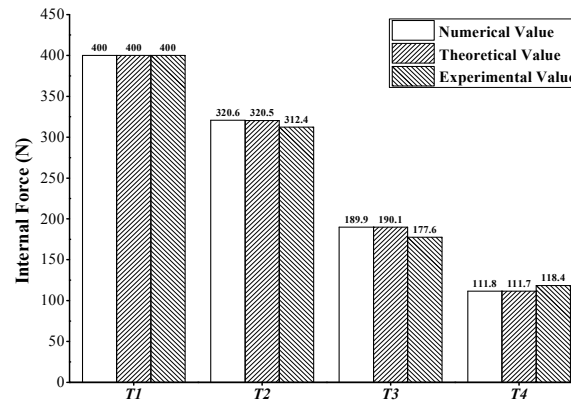


Fig. 14 Comparison of cable forces obtained by different means

model which is comprised of 4 cable segments. As shown in Fig. 13, a dynamometer is installed in the middle of each cable segment to connect the bisected cable segment. A circle ring fixed to the ground is set at each turning point of the cable to simulate the contact of the cable and joint. In the test, a 400 N tensile force was applied at the end of No. 4 cable segment by means of suspended load. Cable forces of each cable segment measured are shown in Fig. 14. The average of coefficients of friction at three turning points calculated is $\mu = 0.26$.

It is indicated in Fig. 14 that theoretical solutions are consistent with numerical solutions which verifies the feasibility of application of the equivalent friction element in continuous sliding cable. As the coefficient of friction is not constant and the average of coefficients of friction is adopted to calculate both theoretical and numerical solutions, the error would occur inevitably. In practice, it is necessary to measure the coefficient of friction between the cable and joint accurately to obtain cable forces with the numerical model presented in this section.

4.3 Truss string structure

In the construction of truss string structure, the continuous cable is usually stretched at one end or at the both ends of the truss, and prestress would transfer in adjacent cable segments through cable-strut joints. The inevitable friction between the cable and joint would result in prestress loss and further the uneven distribution of internal forces of the structure, which would eventually affect the overall performance of the structure. In previous finite element analysis, the continuous cable is simplified as separated cable segments, and each independent cable segment is applied with the same prestress. Obviously, it would result in a great error with the discontinuous cable model, because the effect of frictional loss is ignored and the working principle of discontinuous cable is quite different from that of continuous cable. In this section, the equivalent friction element is applied in the analysis of truss string structure to consider the effect of frictional loss on

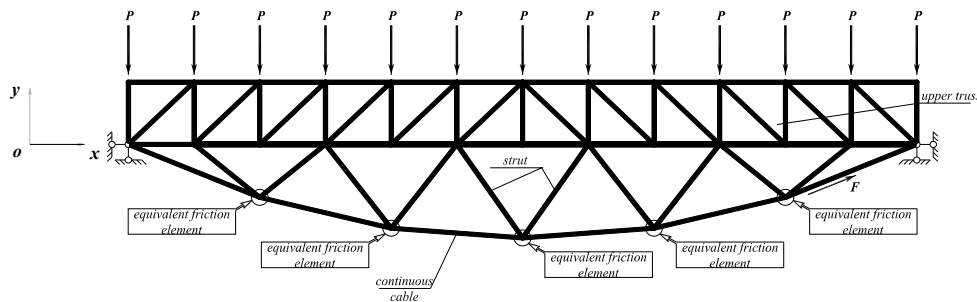


Fig. 15 Truss string structure model

Table 5 List of working conditions considered

Case	Friction coefficient μ	F / kN	Comment
Case 1	0	0	No friction
Case 2	12.7	0	Discontinuous cable
Case 3	0.2	20	Stretch with friction
Case 4	0	20	Stretch with no friction

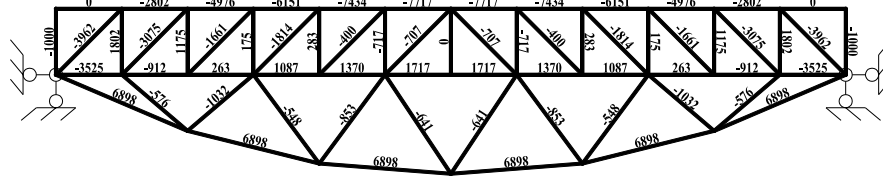
the structure.

A plane truss string structure with a continuous cable is shown in Fig. 15. Equivalent friction elements are established in cable-strut joints. Assume that the modulus of elasticity and the sectional area of all members in the structure are the same with $E = 2 \times 10^5 \text{ N/mm}^2$ and $A = 100 \text{ mm}^2$. An external force F is applied in the tangential direction of the cable at the right end of the cable. The loads and boundary constraints of the truss string structure is shown in Fig. 15, where $P = 1 \text{ kN}$.

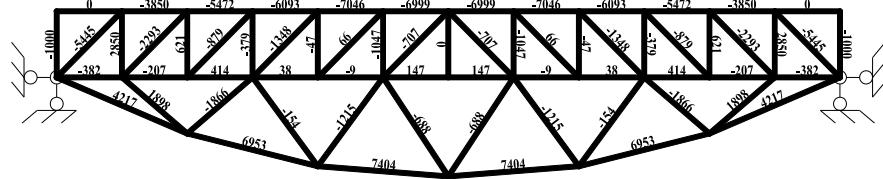
The cable-supported truss was calculated with Matlab, considering the four conditions listed in Table 4. The value of μ in condition 2 is less than the internal friction angle of the cable and the strut joint, and the cable could not slide through the cable-strut joint. In this case, it can be simulated with discontinuous cable model. In addition, the contact friction between the cable and the strut joint could not be considered in MIDAS FEA software, which is a generic commercial finite element software. Therefore, it is the only method to adopt the discontinuous cable model in MIDAS to calculate the cable-supported truss at present. As described above, the discontinuous cable model is equivalent to the case where the friction coefficient is not less than the internal friction angle. Hence, the validity of the equivalent friction element proposed in the paper can be proved indirectly by comparing the results of the condition 2 listed in Table 4 and MIDAS result. The results are shown in Fig. 16. As the continuous sliding cable model is not concluded in Midas and the contact friction between the cable and joint could not be considered in Midas, internal forces in the second condition are also obtained with Midas, shown as Fig. 17.

A comparison of results in Figs. 16(b) and 17 indicates that internal forces calculated by finite element analysis with equivalent friction elements are consistent with Midas results in the second condition $\mu = 12.7$ when the cable could not slide through the joint and equivalent friction elements keep in a fixed state. In addition, results in Fig. 16(a) show that internal forces of all cable segments are equal when there is no friction between the cable and joint. The above results prove the feasibility of equivalent friction elements.

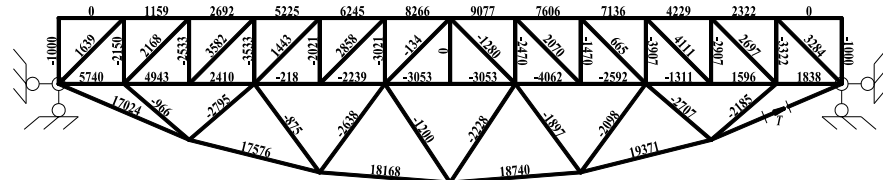
A comparison of Figs. 16(a) and (b) indicates that the distribution of internal forces of the



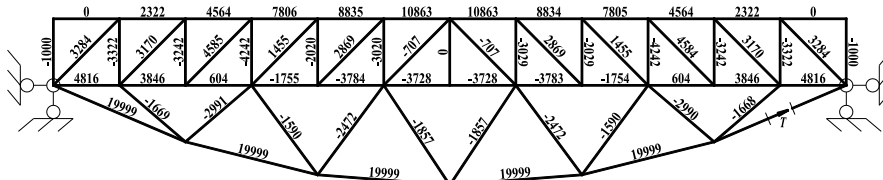
(a) Case 1



(b) Case 2



(c) Case 3



(d) Case 4

Fig. 16 Results of finite element analysis with equivalent friction elements (N)

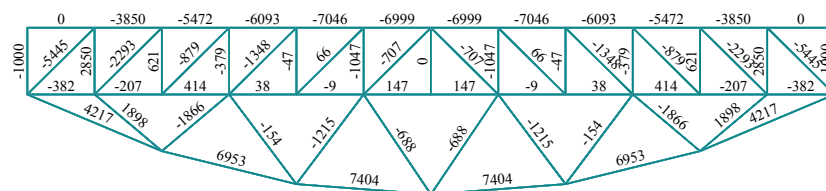


Fig. 17 Results of Midas for the second condition

structure tends to be uneven when the discontinuous cable model is adopted in the analysis of truss string structure. The maximum of cable force with the value of 7,404 N occurs in the cable in the middle of span, while the minimum of cable force is 4,217 N which occurs in the two ends of span,

displaying a significant uneven distribution of cable forces. The maximum and minimum of internal force of struts in the discontinuous cable model are 1,866 N and 154 N respectively, showing a big difference of 1,712 N. Also, tensile force occurs in certain struts. In the continuous cable model, the maximum and minimum of internal force of struts are 1,032 N and 548 N respectively, showing a relatively small difference of 484 N. The above results indicate that the distribution of internal forces in a discontinuous cable model would be more uneven and that the minimum internal force would be underestimated in a discontinuous cable model. There is a similar result in the upper truss. Therefore, there would be a great error if the cable in cable supported structures is signified as discontinuous cable, and internal forces of some members in the structure would be underestimated which is not favored in structural design.

It is indicated in Fig. 16(d) that the internal force distribution in the structure is symmetric when there is no friction. A comparison of results in Figs. 16(c) and (b) shows that the friction between the cable and joint would cause an uneven distribution of internal forces when pretension is applied by means of stretching the cable at one end. Also, Fig. 16(c) indicates that internal forces of struts would decrease when friction exists, which would impair the supporting effect of the cable-strut system on the upper truss. In addition, an uneven distribution of internal forces in the cable-strut system would lead to an uneven distribution of internal forces in the upper truss that internal forces of bars in the truss on the stretching side would decrease while an increase of internal forces would occur in bars on the other side.

Therefore, it is necessary to consider the effect of friction on the structural behavior, since the performance of the structure would be affected by an uneven distribution of internal forces resulted from the friction between the continuous cable and joints.

5. Conclusions

The equivalent friction element is proposed in this paper to consider the effect of friction between the cable and the joint on the mechanical performance of structure. Considering three possible contact state: fixed, sliding and separated, geometric and internal force constraint conditions are determined, and equivalent stiffness matrix and equivalent load vector of the element are derived. The element stiffness matrix and load vector of the equivalent friction element share the same formulation with other finite elements. Hence, the overall analysis of the structure is available by assembling equivalent element stiffness matrixes and equivalent load vectors into global ones. One advantage of the equivalent friction element is that only a few steps of iteration are required to obtain a relatively accurate solution for the analysis considering friction.

Cable-roller model is the fundamental component of the continuous cable in cable supported structures. Equivalent friction element is firstly applied in a cable-roller model, and its feasibility is proved with tensile tests of rolling cable-strut joints. In addition, equivalent friction element is also applied in a continuous sliding cable model. Theoretical values, numerical solutions and experiment results are consistent with each other, verifying the feasibility of equivalent friction element in the continuous sliding cable model.

Finally, equivalent friction element is further applied in truss string structure. Results of the fixed state obtained by finite element analysis with equivalent friction element are compared with Midas results, verifying the feasibility of equivalent friction element again. In addition, there would be a great error if the continuous cable is simplified as the discontinuous one in the finite

element analysis, which should be paid attention to by structural designers. Results also indicate that the structural performance would be affected by the friction between the cable and joints.

Acknowledgments

The authors gratefully acknowledge the support of Independent Innovation Foundation of Tianjin University (Approval No. 1304). The authors would also like to thank the students in the steel research group of Tianjin University for their assistance with the laboratory work.

References

- Aufaure, M. (2000), "A three-node cable element ensuring the continuity of the horizontal tension: a clamp-cable element", *Comput. Struct.*, **74**(2), 243-251.
- Chen, Z.H. (2013), *Beam String Structure System*, Science Press, Beijing, China.
- Chen, Z.H., Wu, Y.J., Yin, Y. and Shan, C. (2010), "Formulation and application of multi-node sliding cable element for the analysis of Suspen-Dome structures", *Finite Elem. Anal. Des.*, **46**(9), 743-750.
- Cui, X.Q. and Guo, Y.L. (2004), "Influence of Gliding Cable Joint on Mechanical Behavior of Suspen-Dome Structures", *Int. J. Space Struct.*, **19**(3), 149-154.
- Cui, X.Q., Guo, Y.L. and Ye, K.M. (2004), "Application of gliding hoop cable joint in suspen-dome structures", *J. Tongji Univ. (Natural Science)*, **32**(10), 1300-1303.
- Katona, M.G. (1983), "A simple contact-friction interface element with applications to buried culverts", *Int. J. Numer. Anal. Method. Geomech.*, **7**(3), 371-384.
- Lei, X.Y. (2001), "Contact friction analysis with a simple interface element", *Comput. Method. Appl. Mech. Eng.*, **190**(15), 1955-1965.
- Lei, X.Y., Swoboda, G. and Zenz, G. (1995), "Application of contact-friction interface element to tunnel excavation in faulted rock", *Comput. Geotech.*, **17**(3), 349-370.
- Li, J.J. and Chan, S.L. (2004), "An integrated analysis of membrane structures with flexible supporting frames", *Finite Elem. Anal. Des.*, **40**(5), 529-540.
- Liu, H.B., Chen, Z.H. and Zhou, T. (2009), "Prestress loss induced by friction in suspensome construction", *J. Tianjin Univ.*, **42**(12), 1055-1060.
- Nie, J.G., Chen, B.L. and Xiao, J.C. (2003), "Nonlinear static analysis of continuous cables with sliding at the middle supporting", *Chinese J. Computat. Mech.*, **20**(3), 320-324.
- Tang, J.M. and Shen, Z.Y. (1999), "A nonlinear analysis with sliding cable elements for the cable structures", *Chinese J. Computat. Mech.*, **16**(2), 143-149.
- Tang, J.M., Dong, M. and Qian, R.J. (1997), "A finite element method with five-node isoparametric element for nonlinear analysis of tension structures", *Chinese J. Computat. Mech.*, **14**(1), 108-113.
- Thai, H.T. and Kim, S.E. (2011), "Nonlinear static and dynamic analysis of cable structures", *Finite Elem. Anal. Des.*, **47**(3), 237-246.
- Wang, S., Zhang, G.J., Zhang, A.L., Ge, J.Q. and Qin, J. (2007a), "The prestress loss analysis of cable-strut joint of the badminton gymnasium for 2008 Olympic Games", *Chinese J. Build. Struct.*, **28**(6), 39-44.
- Wang, Y.Q., Wu, L.L., Shi, Y.J., Sun, F., Luo, K.Y. and Xu, Y. (2007b), "FEM analysis and experimental study on monolayer cable net for glass facades: static performance", *Adv. Struct. Eng.*, **10**(4), 371-382.
- Wang, S., Zhang, G.J., Ge, J.Q., Zhang, A.L. and Guan, Z.Z. (2008), "Influence of prestress loss on structural behavior of the badminton gymnasium for 2008 Olympic Games", *Chinese J. Build. Struct.*, **28**(6), 45-51.
- Wei, J.D. (2004), "Sliding cable element for the analysis of cable structures", *Eng. Mech.*, **21**(6), 172-176.
- Wei, J.D. (2006), "Friction gliding cable element in analysis of gliding cable structures", *Eng. Mech.*, **23**(9), 66-70.

- Wu, Y.J. (2010), *Analysis of Sliding Cable Element and Node*, Ph.D. Thesis, Tianjin University, Tianjin, China.
- Zhang, Z.H. and Dong, S.L. (2001), "Slippage analysis of continuous cable in tension structures", *Spatial Struct.*, **7**(3), 26-31.
- Zhang, G.F., Dong, S.L., Zhuo, X., Guo, J.M. and Zhao, X. (2008), "Research on sliding cable in construction of suspend-dome structures", *J. Zhejiang Univ. (Engineering Science)*, **42**(6), 1051-1057.
- Zhou, B., Accorsi, M.L. and Leonard, J.W. (2004), "Finite element formulation for modeling sliding cable elements", *Comput. Struct.*, **82**(2), 271-280.
- Zhu, M.L., Dong, S.L. and Yuan, X.F. (2013), "Failure analysis of a cable dome due to cable slack or rupture", *Adv. Struct. Eng.*, **16**(2), 259-271.

CC